Design and Implementation of an X-Band Radar System

Lisa Elmiladi, Steffen Kross, Jiuzou Zhang, Cameron Connolly
Department of Electrical Engineering, Colorado School of Mines
Email: lelmiladi@mines.edu, connollyhergert@mines.edu, steffen_kross@mines.edu, jiuzouzhang@mines.edu

***Abstract*—This report presents the design, simulation, and implementation of an X-band radar system on a microstrip PCB. The radar design includes critical components such as hybrid couplers, a 10 dB coupled-line coupler, a third-order Chebyshev bandpass filter, and a balanced mixer. The layout and interconnections were modeled in ADS, and electromagnetic (EM) simulations were performed to validate functionality.**

I. Introduction

Radar systems operating in the X-band (8–12 GHz) are widely used for communication, sensing, and defense applications. This project aims to design and implement an X-band radar using microstrip technology, as shown in Figure 1. The radar architecture includes:

- A 90-degree branchline hybrid coupler for signal splitting.
- A 10 dB coupled-line coupler for LO power reduction.
- A third-order Chebyshev bandpass filter.
- A balanced mixer with matching and DC blocking networks.

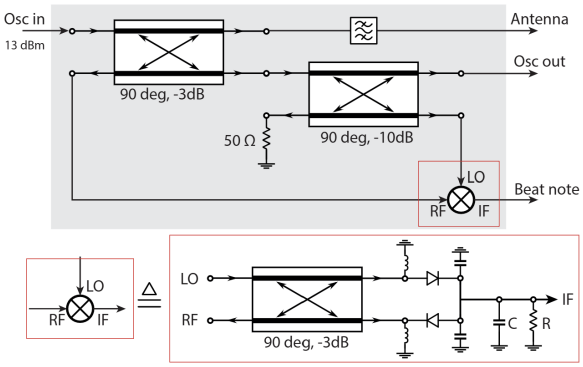

Fig. 1. Radar block diagram.

II. Hybrid Couplers Design

Two hybrid couplers were designed using ADS. Hybrid couplers are critical components in the radar system for power splitting and attenuation. Two designs were implemented: a -3 dB branchline hybrid coupler for signal splitting and recombination, and a -10 dB coupled-line coupler to attenuate the LO power entering the mixer to avoid saturation. Simulations confirmed the desired S-parameter behavior, as shown in Figures 3 and 9. The substrate used for the coupler design was **RO4003**, chosen for its excellent high-frequency performance and compatibility with microstrip line components. This substrate ensures reasonable transmission line spacing for components such as the coupled microstrip coupler, enabling compact and reliable layouts.

-3 dB Branchline Hybrid Coupler Design

The -3 dB branchline hybrid coupler splits input power equally between two output ports with a 90-degree phase difference. This design uses four microstrip transmission lines, modeled in ADS, as shown in Figure 2. The design ensures proper impedance matching and layout integration.

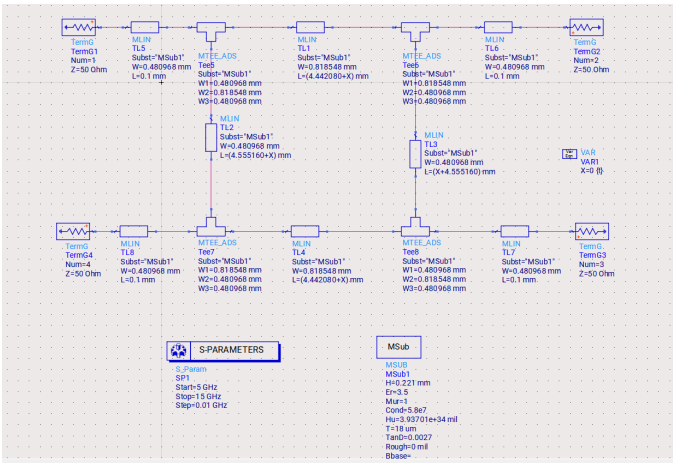

Fig. 2. -3 dB branchline hybrid coupler schematic.

Simulation results confirm the performance:

- Equal power split ($S_{21}, S_{31} \approx -3.019\,\text{dB}$).
- Excellent isolation ($S_{41} \approx -61.465\,\text{dB}$).
- Excellent matching ($S_{11} \approx -40.207\,\text{dB}$).

The magnitude response is shown in Figure 3, while the phase response is depicted in Figure 4. The phase response confirms a 270-degree phase shift between the output ports (S_{21} and S_{31}), validating the coupler's functionality.

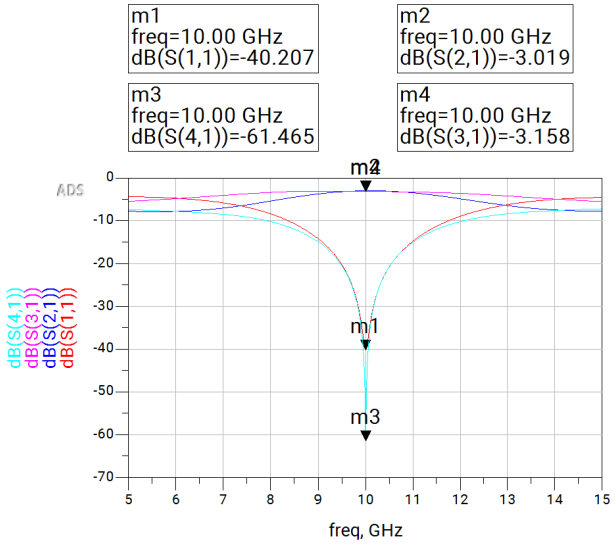

Fig. 3. S-parameter magnitude results for the -3 dB branchline coupler (schematic simulation).

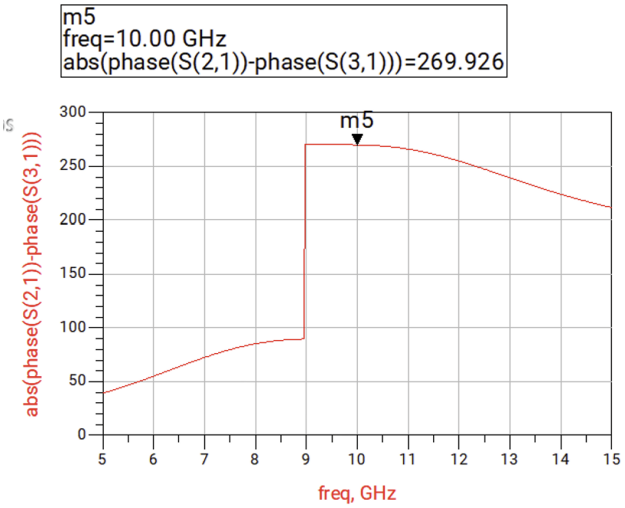

Fig. 4. Phase difference between port 2 and port 3 for the -3 dB branchline coupler (schematic simulation).

Layout and Momentum Analysis

The layout of the -3 dB branchline hybrid coupler, as implemented in ADS Momentum, is shown in Figure 5. The layout ensures compact design and efficient integration with other components in the radar system.

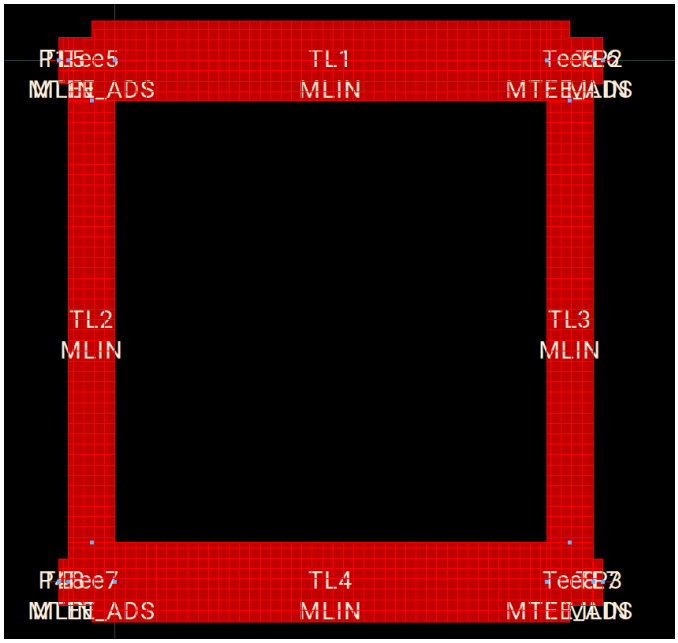

Fig. 5. -3 dB branchline hybrid coupler layout.

Momentum simulations were performed to account for parasitics and substrate effects. These simulations provide a more realistic assessment of the coupler's performance. The magnitude and phase results are shown in Figures 6 and 7, respectively.

The Momentum magnitude results exhibit smoother curves, highlighting reduced numerical artifacts and validating the robustness of the coupler's design in a real-world substrate environment.

Analysis and Observations

The -3 dB branchline hybrid coupler achieves the following:

- Accurate power split with minimal losses.
- Excellent isolation and matching, as confirmed by both schematic and Momentum simulations.
- Compact and practical layout suitable for high-frequency radar systems.

These results validate the design and its implementation, ensuring its effectiveness in the radar system.

-10 dB Coupled-line Hybrid Coupler Design

The -10 dB coupled-line hybrid coupler reduces the power entering the LO port of the mixer to prevent saturation. The schematic of the coupler, modeled in ADS, is shown in Figure 8.

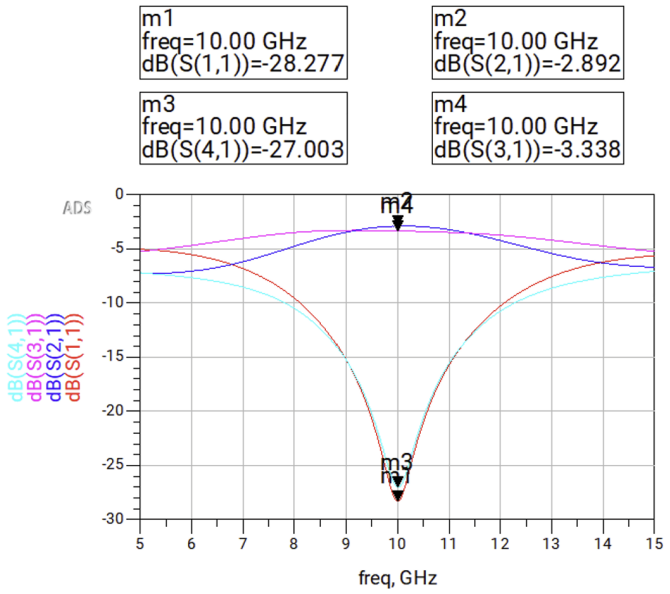

Fig. 6. S-parameter magnitude results for the -3 dB branchline coupler (Momentum simulation).

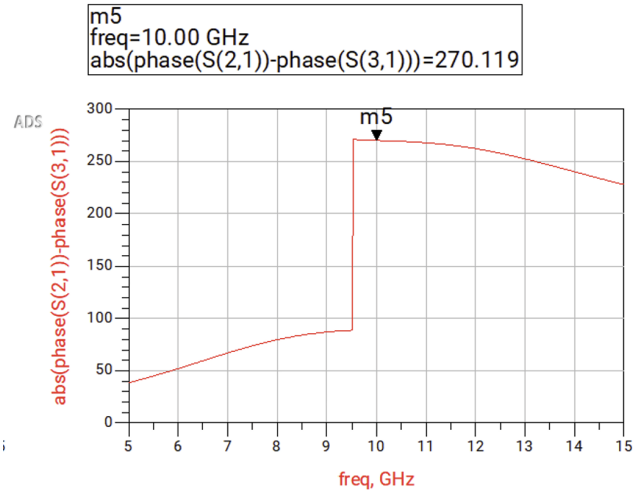

Fig. 7. Phase difference between port 2 and port 3 for the -3 dB branchline coupler (Momentum simulation).

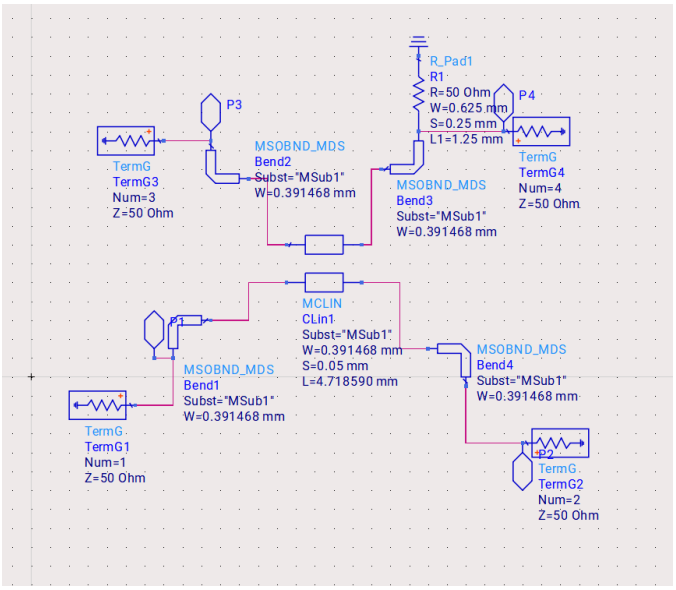

Fig. 8. -10 dB coupled-line hybrid coupler schematic.

Simulation results confirm the design performance:

- Coupling (S_{31}): -10.149 dB.
- Isolation (S_{41}): -20.449 dB.
- Matching (S_{11}): -29.854 dB.

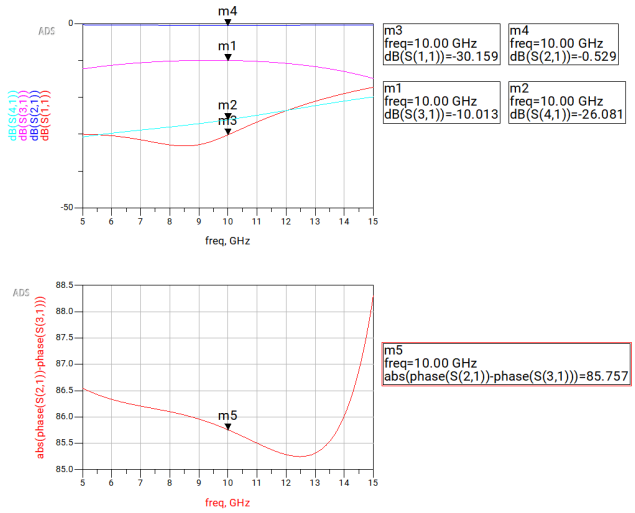

Fig. 9. S-parameter magnitude and phase results for the -10 dB coupled-line coupler.

Layout and Momentum Analysis

The layout of the -10 dB coupled-line hybrid coupler, as implemented in ADS Momentum, is shown in Figure 10. The design integrates compactly and aligns with the specifications for the radar system.

Fig. 10. -10 dB coupled-line hybrid coupler layout.

Momentum simulations were conducted to assess real-world performance, accounting for parasitics and manufacturing tolerances. The results, shown in Figure 11, demonstrate good agreement with the schematic simulations.

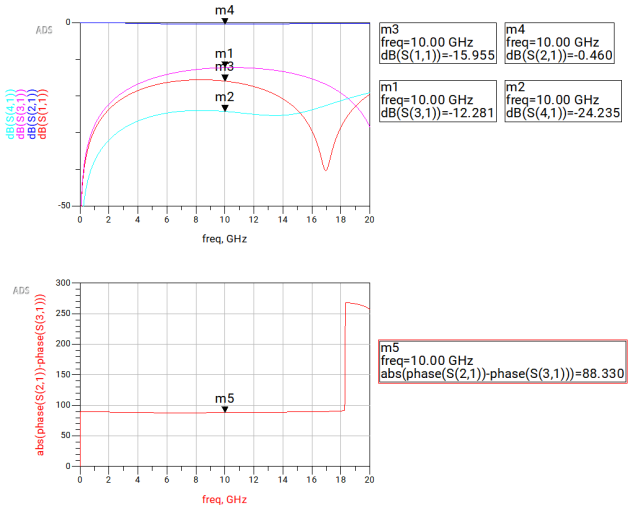

Fig. 11. Momentum simulation results for the -10 dB coupled-line coupler.

Analysis and Observations

The -10 dB coupled-line hybrid coupler achieves the following:

- Accurate coupling to the desired power level of -10 dB, with S(3,1) measured at -12.8 dB, confirming proper attenuation.
- Sufficient isolation and good input matching.
- Compact layout suitable for high-frequency radar applications.

These results validate the -10 dB coupler design for effective integration in the radar system.

III. Chebyshev Bandpass Filter

A third-order Chebyshev bandpass filter with 0.5 dB ripple was designed for the X-band. The design ensures sharp attenuation outside the target frequency range to prevent unwanted radiation.

Design Overview

The schematic of the filter, modeled in ADS, is shown in Figure 12. The design consists of three shunted microstrip lines tailored to the specified bandwidth and ripple. Additional variable parameters (`VAR6`, `VAR7`, and `VAR8`) were introduced to refine the design during the Momentum simulations, enabling precise optimization for EM performance.

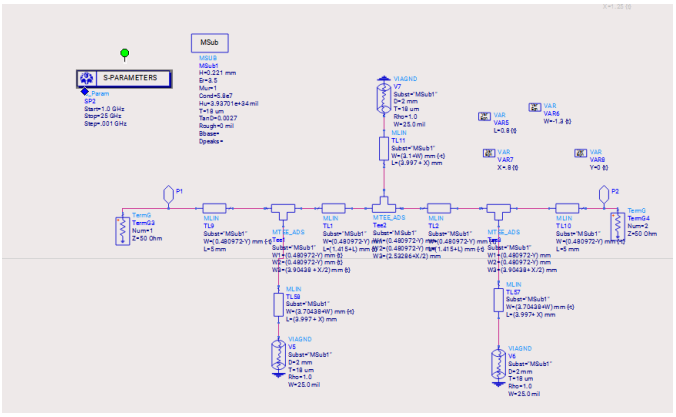

Fig. 12. Chebyshev bandpass filter schematic in ADS.

Simulation Results

The S-parameter simulation results, illustrated in Figure 13, highlight the filter's performance:

- The passband is centered at approximately 10 GHz.
- Insertion loss (S_{12}) in the passband is as low as -0.751 dB.
- Return loss (S_{11}) in the passband remains below -2.447 dB, ensuring efficient transmission with minimal reflection.

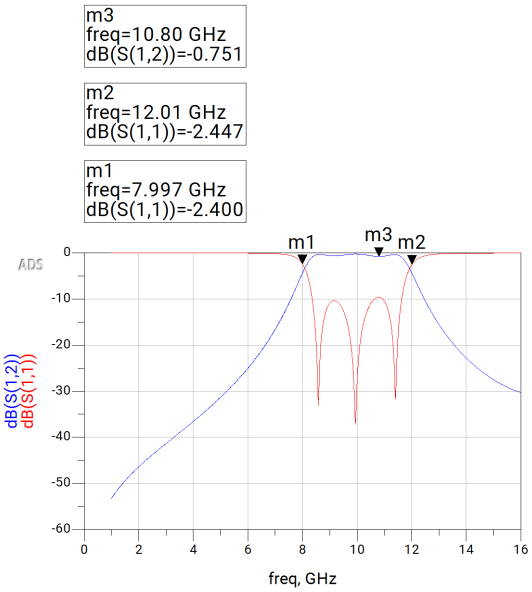

Fig. 13. S-parameter results for the Chebyshev bandpass filter.

Layout and Momentum Analysis

The physical layout of the filter, shown in Figure 14, was designed to accommodate manufacturing constraints while maintaining optimal electrical performance. The Momentum simulation results, shown in Figure 15, confirm the effectiveness of the filter in real-world scenarios, including substrate and parasitic effects.

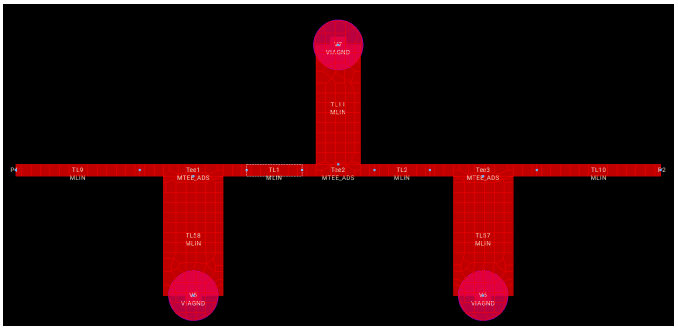

Fig. 14. Physical layout of the Chebyshev bandpass filter.

The Momentum results indicate:

- Smooth S-parameter transitions, validating the design's reliability under real-world conditions.
- Consistent passband characteristics, with slight adjustments from the schematic simulation due to EM effects.

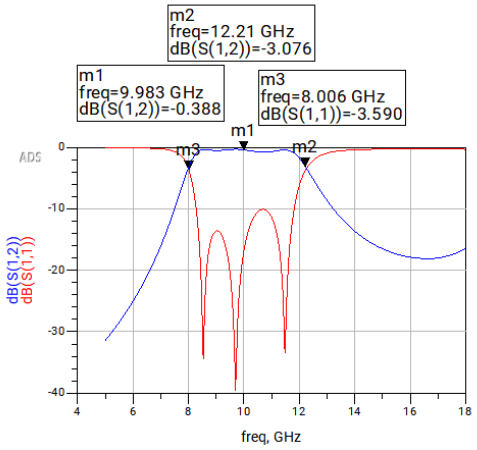

Fig. 15. Momentum simulation results for the Chebyshev bandpass filter.

Performance Analysis

The filter meets the design goals with:

- Precise center frequency tuning through variable parameters.
- Adequate insertion and return loss, ensuring low signal degradation.
- Effective suppression of unwanted frequencies outside the passband.

IV. Balanced Mixer

The balanced mixer is a critical component in the radar system, responsible for frequency conversion. It combines the input RF and LO signals to generate an IF signal, while suppressing unwanted harmonics and ensuring efficient signal conversion. The mixer consists of two main subsections: Subsection A and Subsection B, each tailored for specific functionalities in the design.

A. Subsection A: RF and LO Combination

Subsection A focuses on the initial combination of the RF and LO signals. The design is implemented using Skyworks SMS7630-061 diodes and impedance matching networks. The schematic, layout, and simulation results are as follows:

Schematic and Layout The schematic for Subsection A is shown in Figure 16. The layout, modeled in ADS, is shown in Figure 17. Subsection A contains (from left to right) a branchline coupler for signal mixing, a shorted transmission line in shunt for impedance matching, and a shorted quarter-wavelength transmission line in shunt acting as an RF choke. The final quarter-wavelength transmission line is used in place of the shunted inductor in the given schematic.

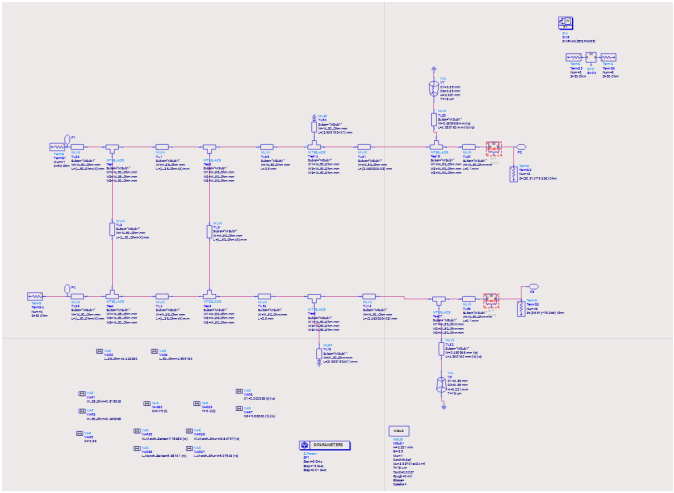

Fig. 16. Schematic of Mixer Subsection A.

Simulation Results S-parameter simulations for Subsection A were conducted to evaluate the performance. The results indicate the RF and LO signals can get through the S2P devices with about 3 dB down and 90 degree phase shift.

These plots provide a clearer visualization of the system's performance in both magnitude and phase, ensuring proper signal combination and minimal interference. The results align with the design criteria, confirming the robustness of the mixer design.

B. Subsection B: IF Signal Filtering and Output

Subsection B handles the LO and RF signal rejections with radial stubs while letting IF signal pass through to the output by combining two branches. The radial stubs are replacing

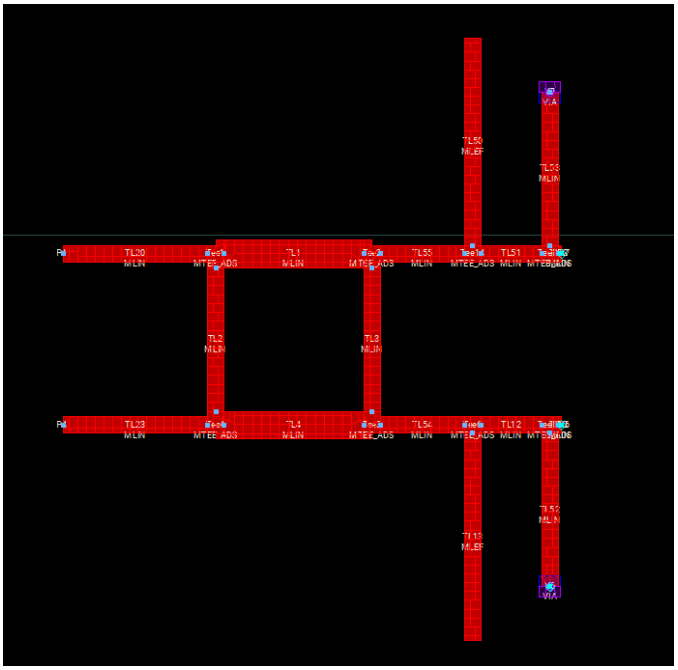

Fig. 17. Layout of Mixer Subsection A.

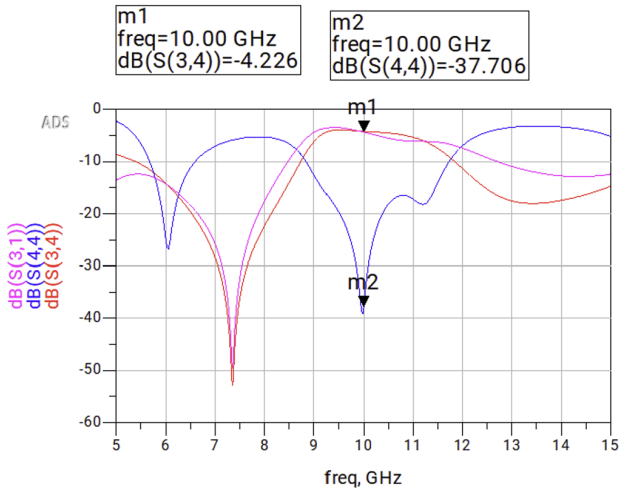

Fig. 18. Magnitude (dB) results for Mixer Subsection A - Schematic Simulation.

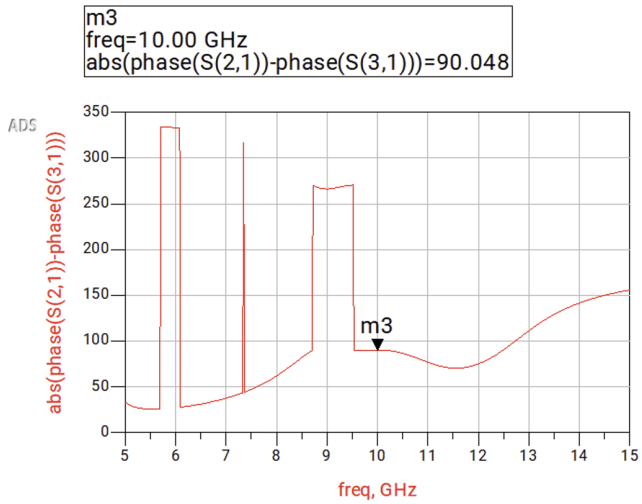

Fig. 19. Phase results for Mixer Subsection A - Schematic Simulation.

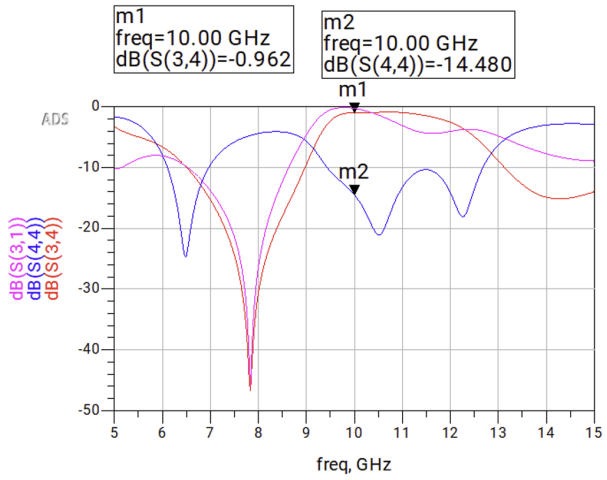

Fig. 20. Magnitude (dB) results for Mixer Subsection A - Momentum Simulation.

the shunted capacitors (DC blocks) in the given schematic. The schematic and layout are shown in Figures 22 and 23. The results were able to verify the radial stubs are working as bandstops. It shows that the RF and LO signals cannot go through the rest of the circuit as they are bandstopped, while the IF signal still can since it is very close to DC frequency and is outside of radial stubs' rejection spectrum.

Simulation Results

Momentum and S-parameter simulations for Subsection B are shown in Figures 25 and 24. Key observations include:

- Smooth IF signal extraction with minimal distortion.
- Excellent harmonic suppression at RF and LO frequen-

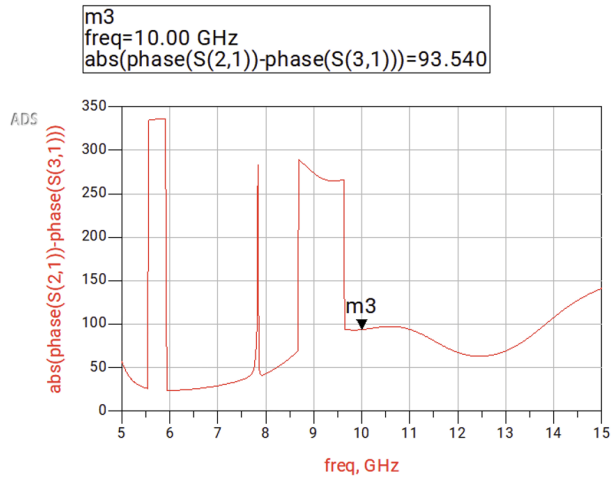

Fig. 21. Phase results for Mixer Subsection A - Momentum Simulation.

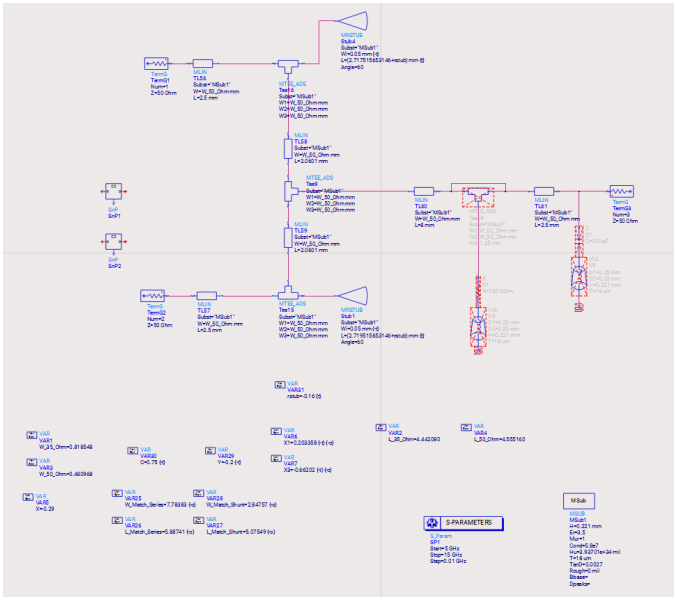

Fig. 22. Schematic of Mixer Subsection B.

cies.

- Acceptable attenuation of higher-order harmonics.

C. Pad Design and Impedance Matching

The Pad section incorporates SMT pads for connecting the diodes and external components, providing impedance matching and stability. The layout and schematic are shown in Figures 26 and 27, respectively. Momentum simulations confirm excellent performance (Figure 28).

D. Diode Network and Impedance Analysis

The diode network is critical for frequency mixing. The impedance of the diode at 10 GHz, shown in Figure 29, en-

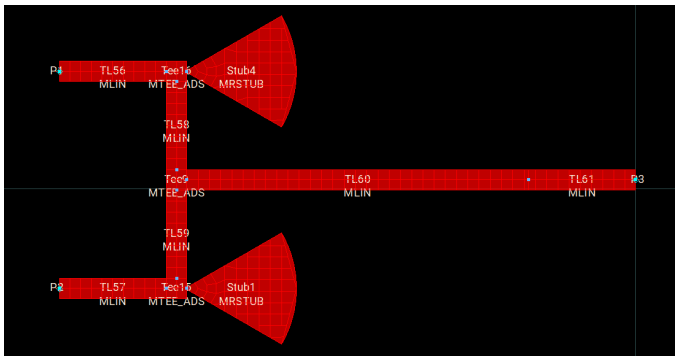

Fig. 23. Layout of Mixer Subsection B.

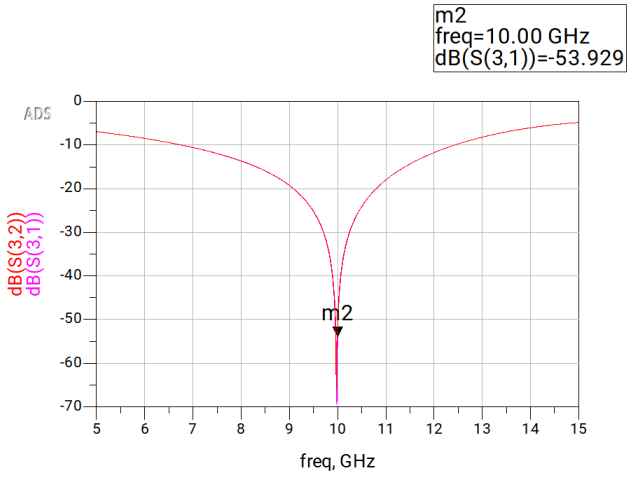

Fig. 24. S-parameter results for Mixer Subsection B.

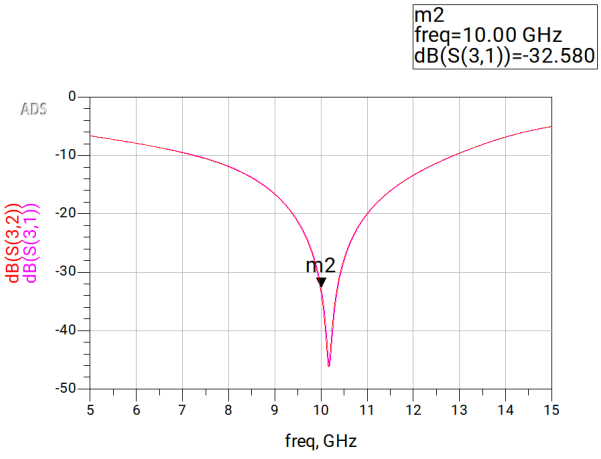

Fig. 25. Momentum simulation results for Mixer Subsection B.

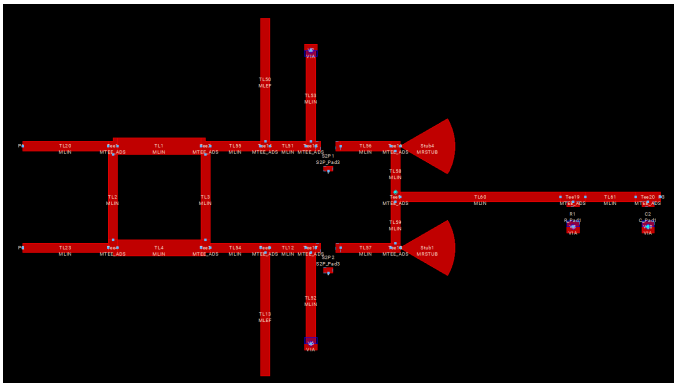

Fig. 26. Layout of the mixer with lumped element pads.

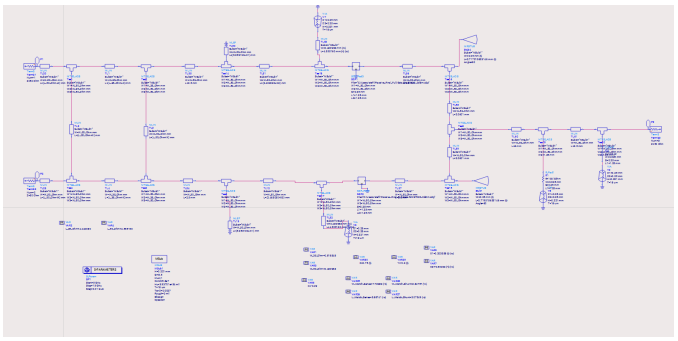

Fig. 27. Schematic of the mixer with lumped element pads.

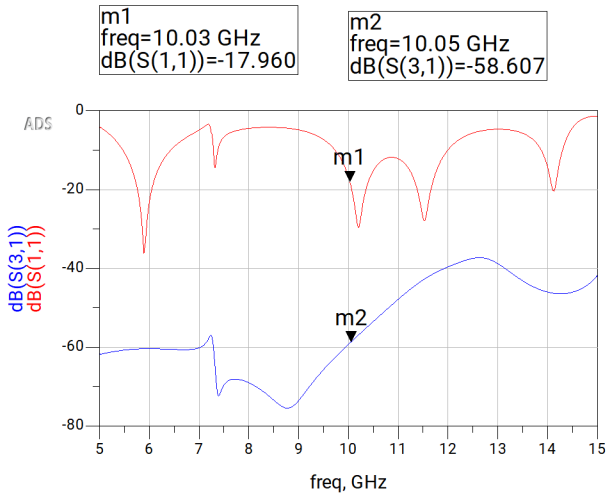

Fig. 28. Momentum simulation results for the mixer with lumped element pads.

sures proper signal interaction. The schematic and simulation results are provided in Figure 30. The network includes:

- RF choke and DC block for diode biasing.
- Tuned impedance matching to the transmission line.

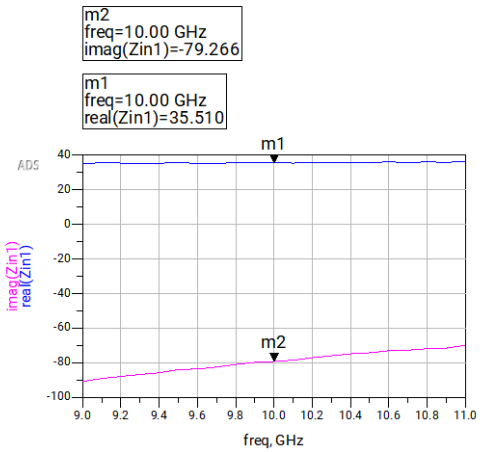

Fig. 29. Impedance of the diode at 10 GHz.

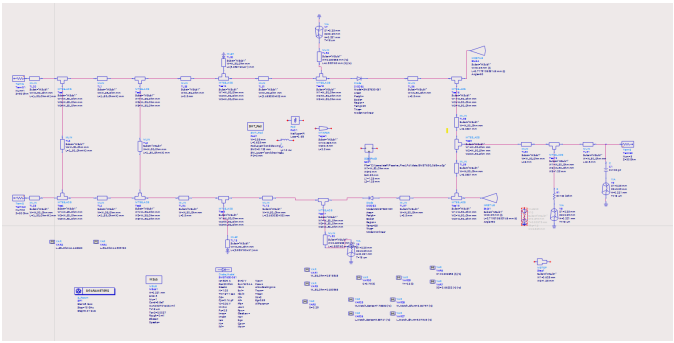

Fig. 30. Schematic of mixer with simulated diodes models.

E. Nonlinear Model with Harmonic Balancing

To further analyze the balanced mixer, a nonlinear model was implemented, replacing the S-parameters with actual diode models. This model allows for more accurate simulation of the mixer's performance, especially for harmonic balance analysis.

1) Design Details

- The nonlinear model uses Skyworks SMS7630-061 diodes for frequency conversion.
- The RF input is represented by an antenna operating at 10 GHz with an input power of -27 dBm.
- The LO input is a single-tone oscillator at 9.99999 GHz (corresponding to 10 kHz IF frequency) with a power level of 13 dBm.

- The IF output frequency of 10 kHz is obtained with an output power of -38.141 dBm.
- Harmonic balancing was employed to analyze the behavior of the mixer across different frequency components.

2) Schematic and Layout

The nonlinear model's schematic and layout are shown in Figures 31 and 34, respectively.

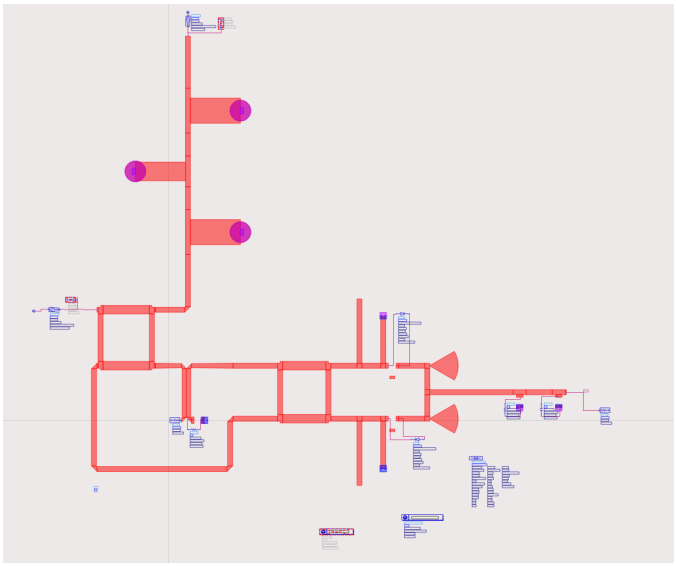

Fig. 31. Schematic of the nonlinear mixer model with harmonic balancing.

3) Harmonic Analysis

The harmonic balance simulation results are shown in Figure 35. The simulation evaluated the output power at the IF port, providing insight into the harmonic components of the output signal.

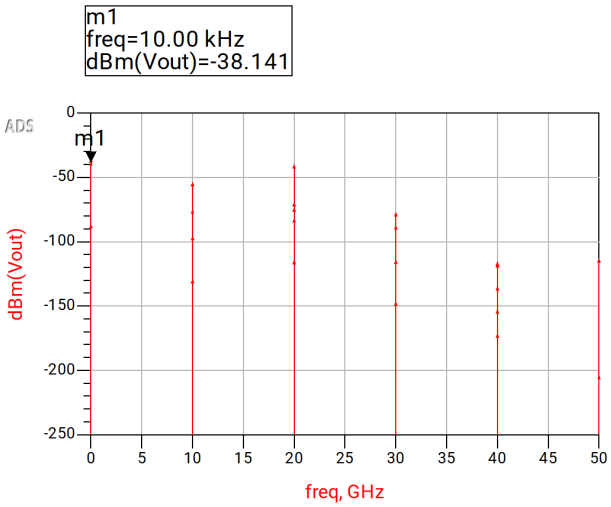

Fig. 35. Harmonic balance simulation results for the nonlinear mixer model.

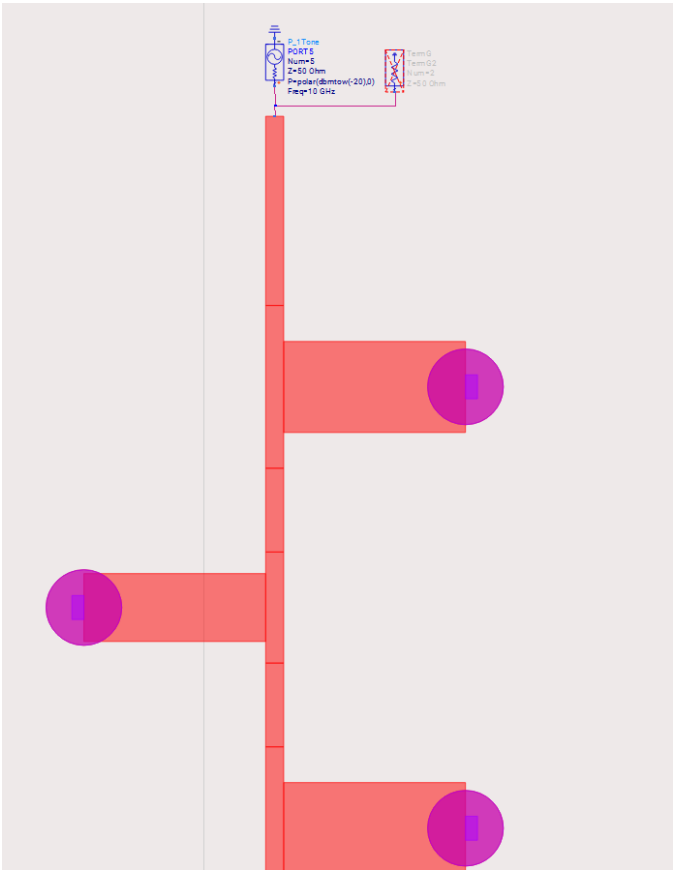

Fig. 32. Nonlinear model input: RF antenna setup at 10 GHz.

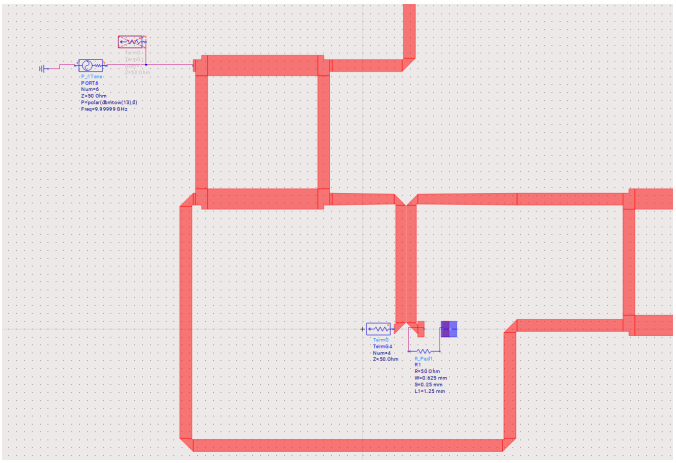

Fig. 33. LO input: Single-tone oscillator setup at 9.99999 GHz.

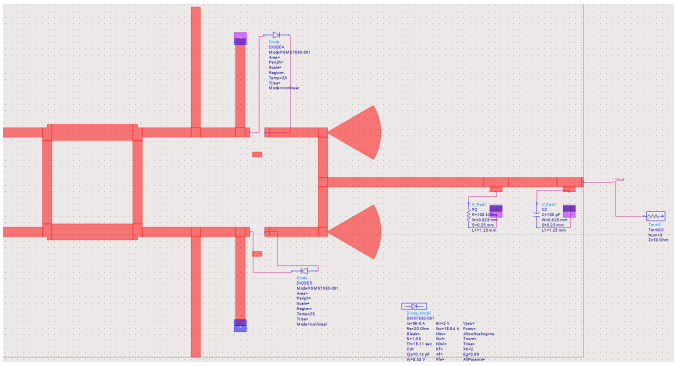

Fig. 34. Layout of the nonlinear mixer model.

4) Key Results

- **IF Output Power**: The IF frequency at 10 kHz exhibits an output power of -38.141 dBm, matching the expected frequency conversion. Given that the RF input is -27 dBm and it goes through the 3dB coupler, the RF signal strength at mixer input is -30 dBm. Hence, the conversion loss is 8 dB (compared with -30 dBm input and driven by 13dBm -3 dB - 10dB = 0 dBm LO signal input).
- **Harmonic Suppression**:
  - RF and LO frequencies (10 GHz and 9.99999 GHz) are sufficiently attenuated.
  - Unwanted harmonics are acceptably suppressed.

V. System Integration and Results

The components were interconnected on a single PCB layout, as shown in Figure 36. Each component was carefully designed and verified individually before integration. The interconnections were implemented with characteristic impedance of 50 Ω at the inputs (Osc in and Antenna) and outputs (Antenna, Osc out, and Beat note). Special attention was given to ensure the layout's integrity and functionality. EM simulations were performed to verify proper functioning, and adjustments were made to ensure optimal performance.

A. PCB Layout and Interconnection

The final layout, shown in Figure 36, integrates all system components. This layout ensures there are no gaps, as confirmed by EM simulation analysis. The layout utilizes 50 Ω transmission lines for all input and output connections, adhering to design requirements.

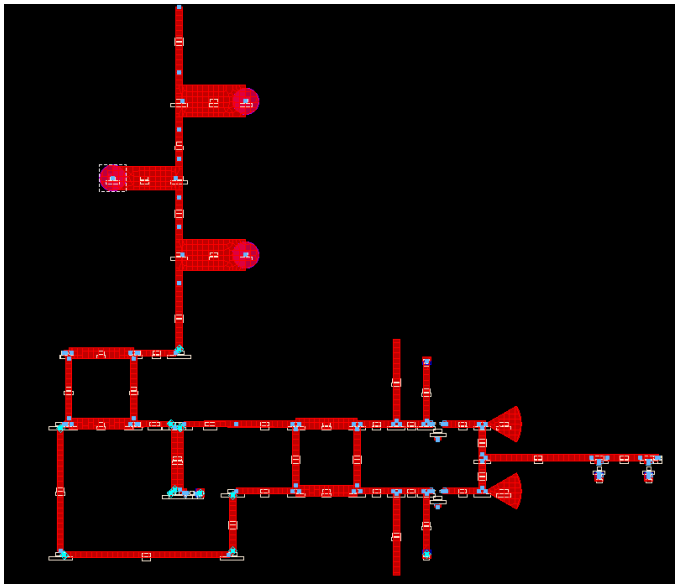

Fig. 36. Final integrated PCB layout with all components interconnected.

B. Schematic of the Full System

The schematic representation of the full system is shown in Figure 37. This schematic highlights the interconnected components, including the oscillator and antenna inputs, mixer, and associated elements.

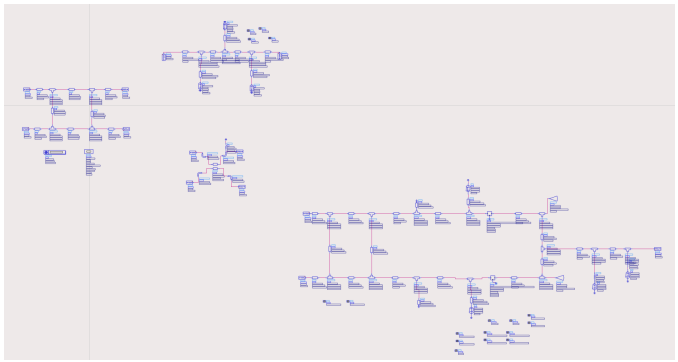

Fig. 37. Schematic of the fully integrated system.

C. Component Integration Verification

Figures 38, 39, and 40 display the individual layouts for the oscillator and antenna inputs, and mixer after final adjustments. The components were designed to ensure smooth integration and proper functionality within the system.

D. Simulation Results

Figure 41 presents the simulation results for the fully integrated system. The plot demonstrates proper frequency conversion, and the LO and RF signals effectively suppressed. Key markers indicate the achieved insertion loss at -52.706 dB for the RF to IF path, -64.979 dB for the LO to IF path, and minimal LO signal leakage at -4.226 dB. In addition, the

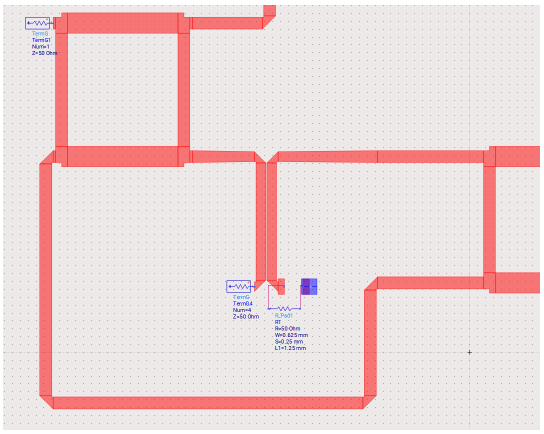

Fig. 38. Final layout of the oscillator component in out port.

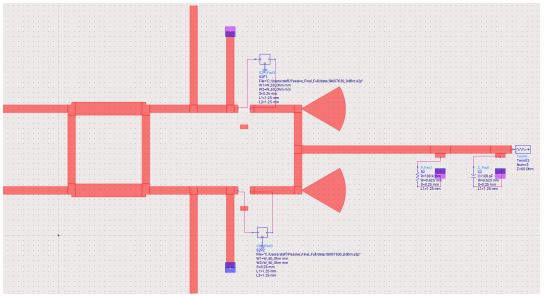

Fig. 39. Final layout of the mixer component.

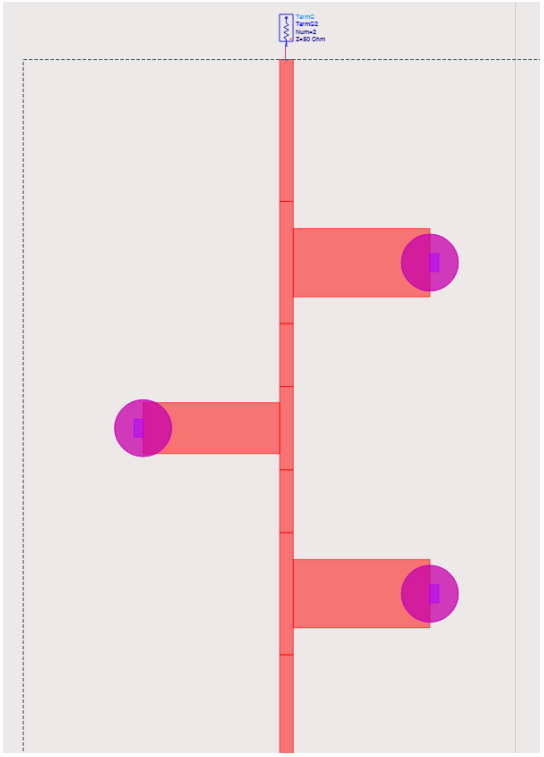

Fig. 40. Final layout of the antenna port and BPF section.

out-of-band (out of 8-12 GHz) signals are sufficiently attenuated. These results validate the design, showcasing effective harmonic suppression, appropriate impedance matching, and overall system functionality in accordance with the design objectives.

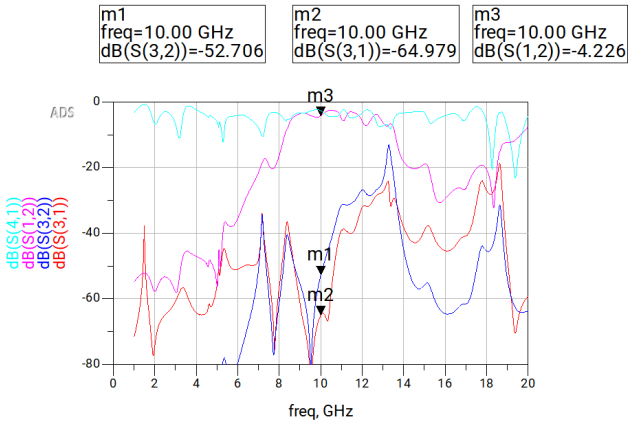

Fig. 41. Simulation results for the fully integrated system, showing proper frequency conversion and harmonic suppression.

E. System Functionality Verification

The EM simulations confirmed the proper functioning of the system layout. Adjustments to transmission line lengths and widths were made where necessary to match the required characteristic impedance. The input and output ports were validated to ensure minimal reflection and maximum power transfer. This integration demonstrates the system's readiness for practical deployment, achieving optimal performance across all metrics.

VI. Extra Credit: SMD Resistor and IF Amplification Stage

This section details the extra credit components added to the radar system design, including the simulation and layout of an SMD resistor connected to the 10 dB coupler and the design of an IF amplification stage using a commercial instrumentation amplifier. The chosen resistor was the RCWP722550R0GKS3 [3]. The S2P file was used to build the design in ADS.

A. SMD Resistor Simulation and Layout

An SMD 50 Ω resistor was connected to the output of the 10 dB coupler. The resistor model includes parasitics (capacitance and inductance) to ensure accurate simulation of real-world behavior. Figure 42 shows the layout including SMA board connectors, while Figure 43 provides the S-parameter simulation results. The design ensures proper impedance matching and minimal reflection at the coupler output.

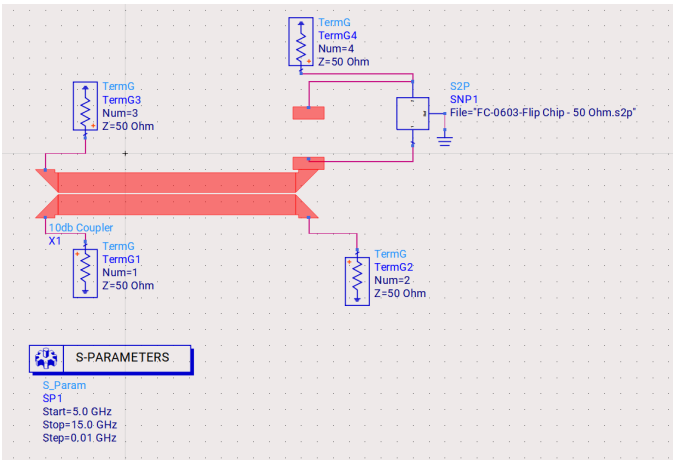

Fig. 42. Layout of SMD resistor connected to the 10 dB coupler.

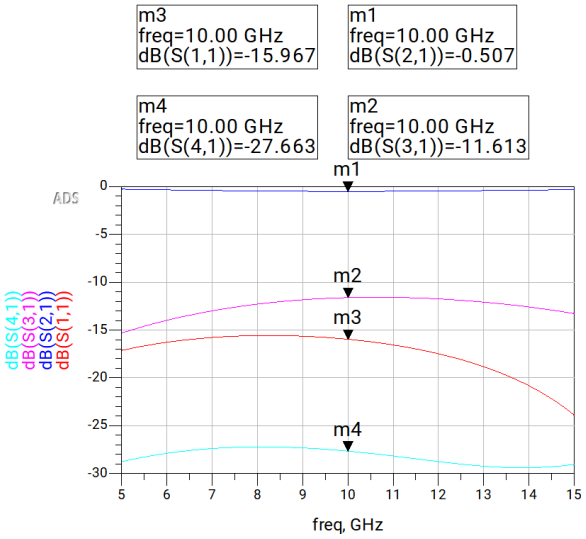

Fig. 43. S-parameter simulation results for the SMD 50 Ω resistor.

The phase behavior of the 10 dB coupler is shown in Figure 44, demonstrating proper phase shift consistency between ports.

B. IF Amplification Stage Design

To amplify the mixer's IF output, the **LT6372-0.2** instrumentation amplifier was selected for its superior performance characteristics:

- Gain: can satisfy 100 V/V.
- Bandwidth: 10 kHz.
- Low noise: 2 nV/$\sqrt{\text{Hz}}$ at 1 kHz.
- Supply voltage: ±15 V.

Design and Layout

The IF amplification stage amplifies the weak 10 kHz IF signal from the mixer, initially at -38 dBm. The amplifier improves the signal to a level suitable for further processing. The input and output are matched to 50 Ω to ensure minimal

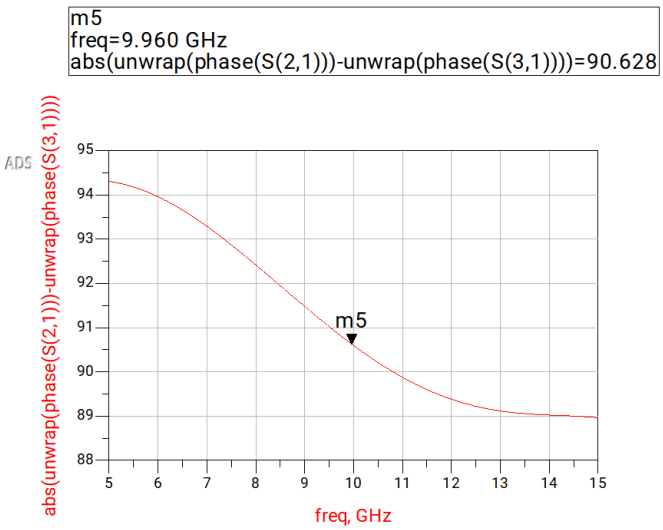

Fig. 44. Phase behavior of the 10 dB coupler.

loss. The layout, including SMA connectors, is shown in Figure 47. The Signal Microwave's ELF40-001 SMA connector was chosen because it supports up to 40 GHz with a reasonably small footprint. The link to this product is in [4]. RFPro simulations were conducted to evaluate the connector's return loss and insertion loss with vias placed under the SMA connectors as shown in Figure 45 . The simulation results confirm excellent signal performance and impedance matching, as shown in Figure 46.

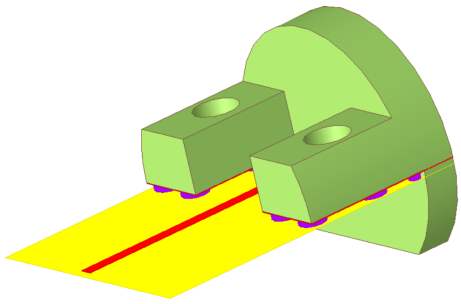

Fig. 45. SMA connector layout with via placement under the connectors.

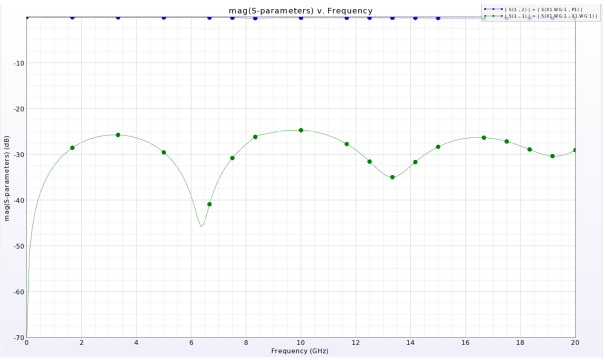

Fig. 46. RFPro simulation results for return loss and insertion loss of the SMA connector.

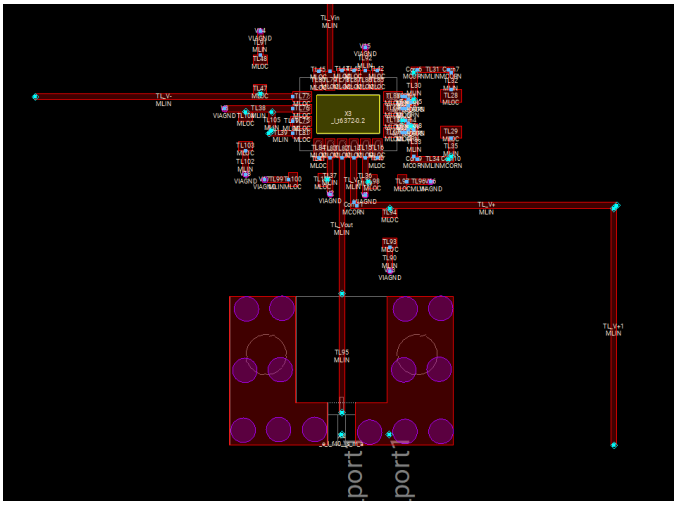

Fig. 47. Layout of the IF amplification stage using LT6372-0.2.

The amplifier circuit simulation, shown in Figure 48, utilizes the LT6372-0.2 instrumentation amplifier. The design includes a gain configuration of 200 V/V, achieved through the precision resistor $R1 = 23.4\,\Omega$ connected between the R_{gf} and R_{gs} pins. The simulation indicates a gain of 150 V/V, indicating an approximate 3dB gain compression, but still exceeding the required 100 V/V. The power supply is provided by $V_1 = +15\,\text{V}$ and $V_2 = -15\,\text{V}$, ensuring the amplifier operates within its specified voltage range. The input signal is generated using a sinusoidal source V_4, which provides a 10 kHz signal with a 1 µV amplitude. This low-level signal demonstrates the amplifier's ability to handle weak signals. A bypass capacitor $C_2 = 0.1\,\mu\text{F}$ is connected across the supply rails for stability, while $C_1 = 0.1\,\mu\text{F}$ is added to ensure supply rail stability. For lumped component sizes, the gain resistor R1 is of 0603, while capacitors are of 0402. The output is matched to a 50 Ω load resistor R_2, ensuring compatibility with subsequent stages in the signal chain. The reference pins (Ref1 and Ref2) are connected to ground, maintaining a stable reference point for single-ended input signals. This configuration ensures accurate amplification of the IF signal while minimizing distortion and noise.

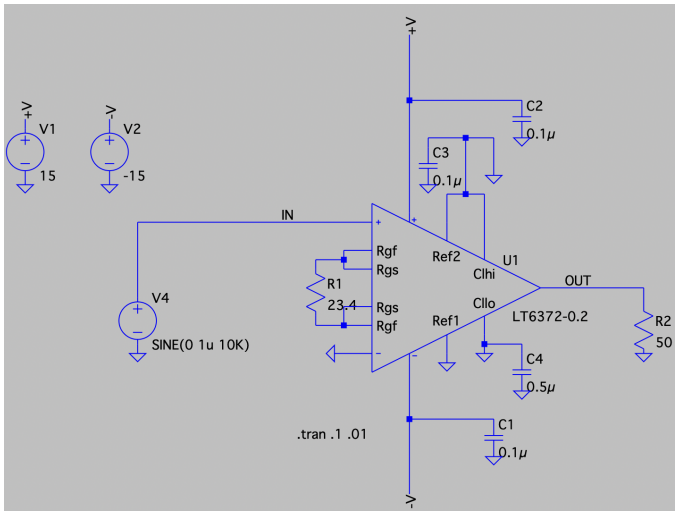

Fig. 48. LTSpice simulation of the IF amplifier using LT6372-0.2, highlighting key components and connections.

For the $23.4\,\Omega$ resistor, the CPF0603B24R3E1 was chosen [5], a high-precision resistor with 0.1% tolerance, to ensure gain accuracy for our IF amplifier. Its 0603 footprint is suitable for compact layouts. For the $0.1\,\mu$F capacitor, the C0402C104K4RAC3121 was selected [6], as it provides excellent performance for decoupling applications and has a reasonable 0402 footprint for efficient integration. The importance of decoupling capacitors is highlighted in [7], which provides a detailed explanation of the current flow differences with and without decoupling. Proper placement of decoupling capacitors close to the power supply pins ensures a short ground return path, significantly reducing transient effects and improving the reliability of high-frequency amplifier designs. The simulation results for the IF amplifier are shown in Figure 49, confirming proper signal gain and bandwidth.

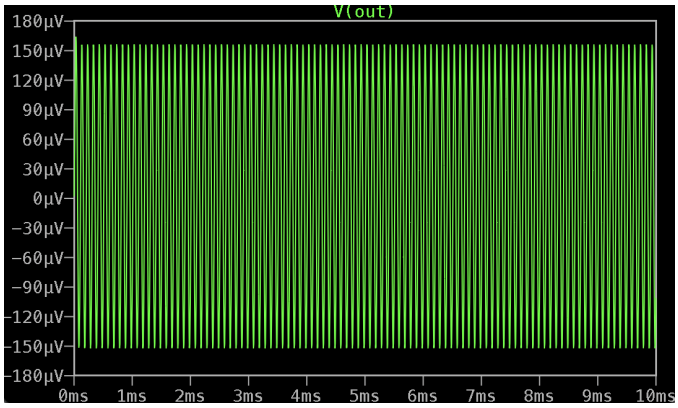

Fig. 49. Simulation results for the IF amplifier using LT6372-0.2.

C. Top and 3D Views of Integrated Design

Figures 50 and 51 provide the top-down and trimetric views of the final amplifier and system integration, demonstrating clear interconnections.

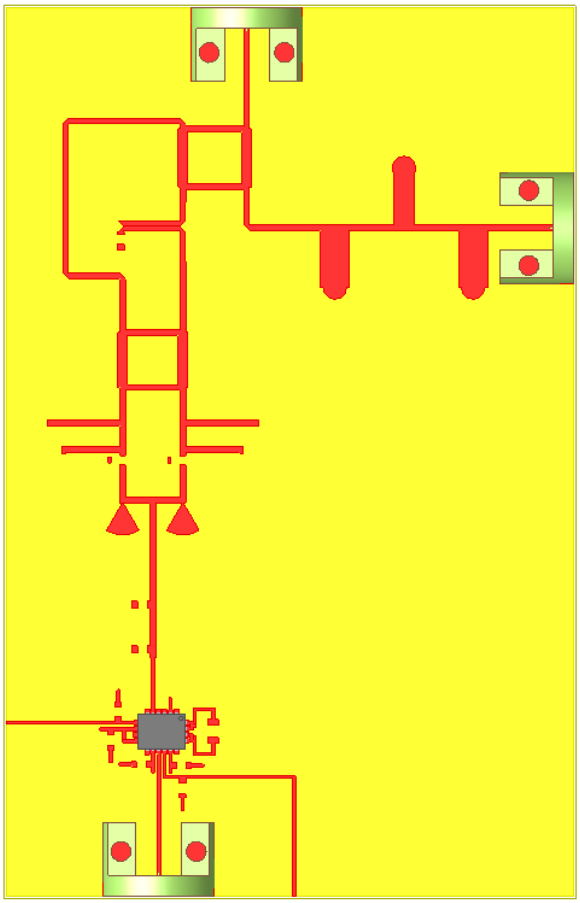

Fig. 50. Top-down view of the amplifier stage layout.

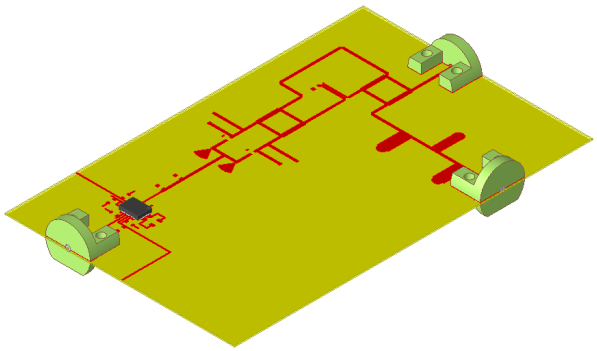

Fig. 51. Trimetric view of the amplifier stage layout.

The via view of the IF amplifier is included in Figure 52, showcasing the interconnections within the PCB layers.

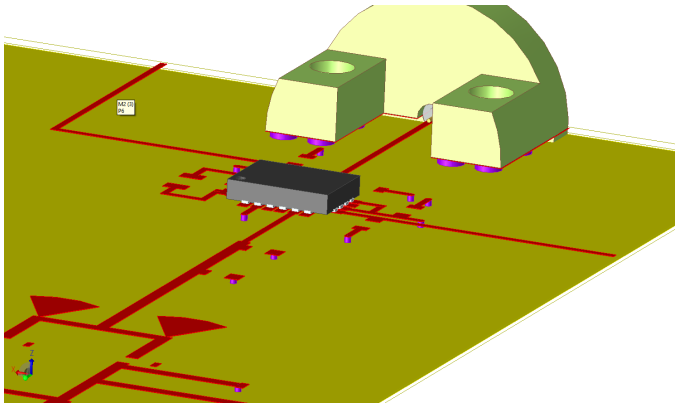

Fig. 52. Via view of the IF amplifier layout.

VII. Conclusion

The X-band radar system was successfully designed, simulated, and validated, achieving the project objectives with all components functioning as intended. The design incorporated a balanced mixer, a 10 dB coupler, and an IF amplification stage, each optimized for minimal signal loss, proper impedance matching, and some harmonic suppression. Electromagnetic (EM) simulations verified layout integrity, while the inclusion of parasitics ensured accurate modeling of real-world behavior.

The integration of all components on a single PCB demonstrated seamless operation and compliance with the design specifications. The SMD 50 Ω resistor and instrumentation amplifier were effectively implemented, with the amplifier enhancing weak IF signals to levels suitable for further processing. The final layout, supported by detailed simulation results, confirmed proper frequency conversion, phase behavior, and signal amplification across the system.

Future work includes the fabrication of the design, experimental testing to validate simulation results, and optimization for further performance improvements, such as reducing noise and increasing dynamic range. The project provides a robust foundation for developing advanced radar systems and highlights the potential for scaling and adaptation to other applications.

References

[1] Advanced Design System (ADS), Keysight Technologies. [Online]. Available: https://www.keysight.com/

[2] Skyworks Solutions Inc., “SMS7630-061 Diode Datasheet”. [Online]. Available: https://www.skyworksinc.com/

[3] Vishay Thin Film, ”FC0603E50R0BST1 Resistor,” https://www.mouser.com/ProductDetail/Vishay-Thin-Film/FC0603E50R0BST1?qs=DyUWGjl%252BcVtp3ZbCgGaMbw%3D%3D. Accessed: December 5, 2024.

[4] Signal Microwave, ”2.92mm Edge Launch Connectors,” https://signalmicrowave.com/2-92mm-edge-launch-connectors. Accessed: December 5, 2024.

[5] TE Connectivity Holsworthy CPF0603B24R3E1 Resistor. https://www.mouser.com/ProductDetail/TE-Connectivity-Holsworthy/CPF0603B24R3E1?qs=sGAEpiMZZMtG0KNrPCHnjay8%2FFDDpf%252B%2FpdjbtTEJJiA%3D.
[6] KEMET C0402C104K4RAC3121 Capacitor. https://www.mouser.com/ProductDetail/KEMET/C0402C104K4RAC3121?qs=jI8Gez59nxKawVwcGEkjIA%3D%3D.
[7] Texas Instruments. "The Decoupling Capacitor: Is it Really Necessary?" https://e2e.ti.com/blogs_/archives/b/precisionhub/posts/the-decoupling-capacitor-is-it-really-necessary.